

# Liquefaction susceptibility of silty tailings under monotonic triaxial tests in nearly saturated conditions

Gianluca Bella\*<sup>1</sup> and Guido Musso<sup>2</sup>

<sup>1</sup>Pini Group SA, Via Besso 7, Lugano, Switzerland

<sup>2</sup>Politecnico di Torino, C.so Duca degli Abruzzi 24, Torino, Italy

(Received April 26, 2023, Revised September 27, 2023, Accepted January 3, 2024)

**Abstract.** Tailings are waste materials of mining operations, consisting of a mixture of clay, silt, sand with a high content of unrecoverable metals, process water, and chemical reagents. They are usually discharged as slurry into the storage area retained by dams or earth embankments. Poor knowledge of the hydro-mechanical behaviour of tailings has often resulted in a high rate of failures in which static liquefaction has been widely recognized as one of the major causes of dam collapse. Many studies have dealt with the static liquefaction of coarse soils in saturated conditions. This research provides an extension to the case of silty tailings in unsaturated conditions. The static liquefaction resistance was evaluated in terms of stress-strain behavior by means of monotonic triaxial tests. Its dependency on the preparation method, the volumetric water content, the void ratio, and the degree of saturation was studied and compared with literature data. The static liquefaction response was proved to be dependent mainly on the preparation technique and degree of saturation that, in turn, controls the excess of pore pressure whose leading role is investigated by means of the relationship between the -B Skempton parameter and the degree of saturation. A preliminary interpretation of the static liquefaction response of Stava tailings is also provided within the Critical State framework.

**Keywords:** CSL; degree of saturation; preparation technique; static liquefaction; suction; unsaturated soil; void ratio

## 1. Introduction

Tailings are waste products resulting from mining processes, usually retained within storage facilities, also known as tailing dams. Depending on the solid/liquid ratio that derives from the handling given to the slurries at the end of the separation processes of mineral extraction, tailings have the consistency of a slurry, cake, or paste. Tailing dams usually consist of a basin and a raised embankment built over time. According to the adopted deposition method, a lower permeability zone made of fine particles would exist far from the dam (decant pond), a high permeability zone made of coarse sediments is placed close to the embankment/discharge point and, between them, there is a transitional zone with an intermediate permeability (beach). The position of the phreatic surface within tailing storage facilities is governed by several external factors due to the interactions with the atmosphere.

The infiltration rate, the amount of surface runoff, or consolidation process are the main external factors that lead to variations in position of the water table, and so the height of the unsaturated zone within the basin (Carrier 1991, Alonso and Gens 2006, Bhanbhro 2014, Zuoan *et al.* 2019). About 25% of failures are related to the static liquefaction phenomena triggered by intense rainfall or rapid snowmelt (Rico *et al.* 2008). Indeed, it is essential to have a deep

understanding of the unsaturated conditions within the tailing dams arising from atmospheric interactions to perform stability analyses that account for the behavior of tailings in unsaturated conditions. Furthermore, issues deriving from poor embankment management should also be considered (Horn *et al.* 2018, Deng *et al.* 2020, Girardi and Bella 2023). The latter (i.e., poor maintenance of the drainage structures or fast dam rise) is the second reason for collapses, while seepage, piping, overtopping, and dynamic liquefaction are additional common causes of collapse. It is also worth noting that the construction scheme of tailing dams (full scheme) is prone to triggering local failures, not only depending on a small scale (specimen scale). Indeed, heterogeneity due to the tailings deposition technique, position, and extent of horizontal layers of fine tailing layers represents relevant factors potentially related to local failures and impacting the dam stability (Becker *et al.* 2023, Whittle *et al.* 2022, Morgenstern *et al.* 2016). Finally, the high number of worldwide collapses involving both active or closed tailing facilities is raising serious environmental threats, since the released tailings flow downstream as viscous fluids with consequences in terms of loss of lives, environmental pollution, and property damages (Fig. 1(a) and 1(b)).

Moving from these reasons, this study gives the main overcomes of an experimental campaign to investigate the static liquefaction response of tailings in unsaturated conditions which, when modeled numerically will result in a more accurate evaluation of the tailing dam safety. This paper aims to investigate the behavior of tailings with respect to their susceptibility to undergo static liquefaction

---

\*Corresponding author, Ph.D.  
E-mail: gianluca.bella@pini.group

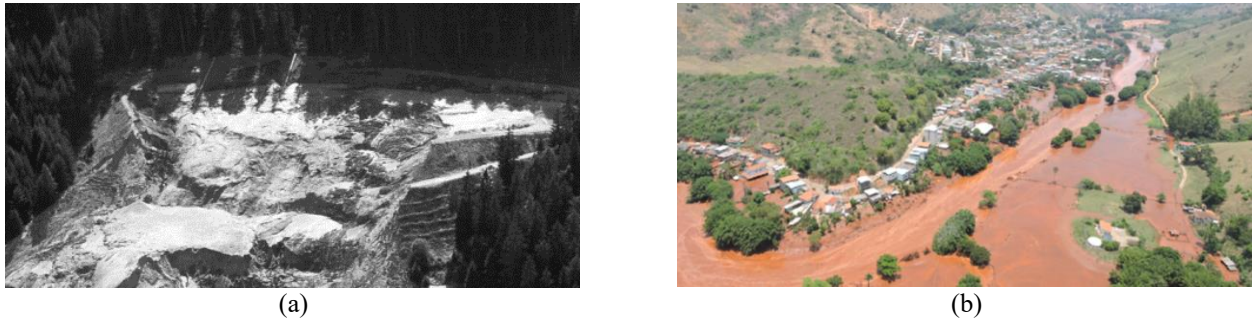


Fig. 1 (a) Stava tailing dams – Italy, 1985 (Lucchi 2020) and (b) aerial view of buildings damaged by the collapse of the Fundão tailings dam – Brazil, 2015 (Carmo *et al.* 2017).

in conditions close to saturation. Indeed, previous experimental studies investigated the failure susceptibility of such soils under saturated conditions (Carrera 2008, Carrera *et al.* 2011), while numerical analyses were carried out to investigate their post-failure behaviour (Pirulli *et al.* 2017). On the basis of the outcomes provided by Carrera (2008) and Carrera *et al.* (2011), the current study investigates the effects of those factors whose relevance is already demonstrated for quartzitic sands. The influence of the preparation technique, the volumetric water content, the degree of saturation, and the void ratio on the static liquefaction response was evaluated by means of monotonic triaxial tests under undrained conditions. The experimental campaign was carried out on silty samples collected from the Stava basins and finds its practical application for reliably assessing the stability of tailing dams, therefore improving their safety from the design to the closure.

## 2. Susceptibility to liquefaction under saturated and unsaturated conditions: state-of-the-art

In geotechnical engineering, ‘liquefaction’ describes a complete loss of strength that occurs when the pore pressure of a saturated soil equals the mean total stress, bringing the effective stress to zero (Olson *et al.* 2000). The effects of liquefaction are devastating since liquefied tailings are released into the environment in form of a heavy liquid, much denser than water (Zeybek 2022). Liquefaction risk assessment represents a relevant issue in geotechnical engineering since it deals with complex deformation mechanisms due to the temporary change of the soil from a solid to a fluid state. (Flora *et al.* 2023). In the case of contractive soils, static liquefaction can be induced by the sudden changes in total stress under undrained conditions, i.e. erosion of the dam toe, overtopping, internal erosion, or collapse of foundation (e.g., Leong *et al.* 2000, Wanatowski and Chu 2007). With reference to tailing dams, fast external loading can be represented by an excessive dam rising rate. More in general, liquefaction can also be caused by changes in the hydraulic conditions of the site, such as an increase of the phreatic table caused by unusual rain, snowmelt, drainage system failure, and other processes that can result in an increase in pore water pressure while the vertical load remains unchanged. If the trigger is an external load, the static liquefaction can be studied by performing

consolidated triaxial test with shearing under undrained conditions (CU), while a constant shear triaxial test (CS) under drained conditions can be performed if the trigger is the increase in pore pressure under constant total stress (Gajo *et al.* 2000, Chu *et al.* 2003, Daouadji *et al.* 2010). In recent years, laboratory tests have shown that not only saturated soils, but also unsaturated soils can be prone to liquefy.

Unno *et al.* (2006) studied the role of suction on the cyclic behavior of unsaturated volcanic sandy soils: they concluded that the air entry value of the soil would be a key parameter in the liquefaction mechanism. For the samples with initial suction above the air entry value, liquefaction was not observed.

Tsukamoto *et al.* (2014) investigated the cyclic response of partially saturated silty sand and showed that liquefaction was unlikely to occur under an initial saturation degree ranging from 0.40 to 0.70. The cyclic behavior of fully saturated and unsaturated fine sand was then explored by Zhang *et al.* (2016) and Vernay *et al.* (2017; 2018), observing an increase in liquefaction occurrence when the degree of saturation increases.

Okamura and Soga (2006) performed undrained triaxial tests on Toyoura sand and showed that decreasing the degree of saturation leads to better liquefaction strength. Similar results were recently obtained by Marabet *et al.* (2019) based on undrained triaxial tests on natural Chlef sand under different initial densities, confining pressure, and Skempton coefficient  $B$ . Again, the Authors observed that the decrease of  $B$  induces a decrease of pore water pressure and an increase of the shear strength. These results are confirmed by Abdallah *et al.* (2021) who performed a series of undrained triaxial tests on unsaturated Chlef sandy samples.

In the frame of the liquefaction susceptibility, the sample volume change represents an issue recently investigated. Depending on the absolute pore water pressure, the degree of saturation, and the initial confining stress, the potential volumetric strain has been used to quantify the liquefaction potential of soil (Okamura and Soga 2006, Unno *et al.* 2008), despite additional studies proved that this approach may be not conservative (Wang *et al.* 2016). The effects of the degree of saturation on the volumetric response of the soil were then investigated by Tsukamoto (2019), suggesting that the cyclic-loaded samples could not liquefy if the saturation degree was lower

than 0.70. Some additional investigations demonstrated that the potential volumetric strain can be used into an approach based on the dissipated energy to predict the soil liquefaction. The effects of the initial stress on the volumetric strain have been also studied by Mele *et al.* (2019b, 2021), concluding that the liquefaction strength of unsaturated soils is related to the specific energy spent to liquefaction, including the contribution of the energy needed to compress the air bubble into the sample and the energy need to liquefy the soil. Recently, Tran *et al.* (2023) performed a series of triaxial tests on unsaturated medium-dense Hostun RF sand. They observed a great difference in the soil behaviour of samples having a degree of saturation up or below 0.95, concluding that the increasing of pore water pressure in combination with variations in volumetric strain is a reason leading failure.

Finally, the effects of the unsaturated conditions have been investigated to develop promising ground improvement techniques against liquefaction, i.e., the Induced partial saturation IPS, as recently shown by several Authors (Mele *et al.* 2019a, Mele *et al.* 2019b, Wang *et al.* 2016, Tsukamoto *et al.* 2014) with some promising in-situ applications (Nagao *et al.* 2015, Okamura *et al.* 2010).

All of this evidence from the literature shows that the susceptibility to static liquefaction of non-plastic soils is influenced by their specific volume and by the amount of stored water (i.e., for unsaturated conditions, by the degree of saturation  $S_r$  and the water ratio  $e_w$ ). This aspect might be particularly relevant for the stability of the tailing dams, especially in the area of the decant pond, where finer materials are disposed. Their water retention behavior allows the existence of a thicker vadose (unsaturated) zone with respect to the one of the dam so that a larger mass of water is stored here.

### 3. Testing material

#### 3.1 Material characterization

The static liquefaction response of Stava tailings was investigated by means of an experimental campaign carried out on unsaturated samples from the lower portion of the Stava upper dam. Built one above the other on a natural slope near the municipality of Stava, Italy (Fig. 2), the two tailing dams were gradually raised to store the waste products coming from the separation floatation process of the Prestavel fluorite mine. In July 1985, the upper tailing dam collapsed on the lower one which, in turn, failed triggering a 250'000 m<sup>3</sup> flow-slide spilled out at an estimated speed of 90 km/h, leading to 268 casualties and extensive environmental and economic damages. Poor drainage, high phreatic level, and unconsolidated state of the stored tailings are supposed to be the main factors that lead to the static liquefaction and the failure of the Stava tailings dam (Davies *et al.* 2000, Lucchi 2015). The material investigated in this study is the fraction passing through ASTM sieve N 200 of the Stava tailings. Its grain size distribution is given in Fig. 3: the clay fraction is 8% of the total solid mass.

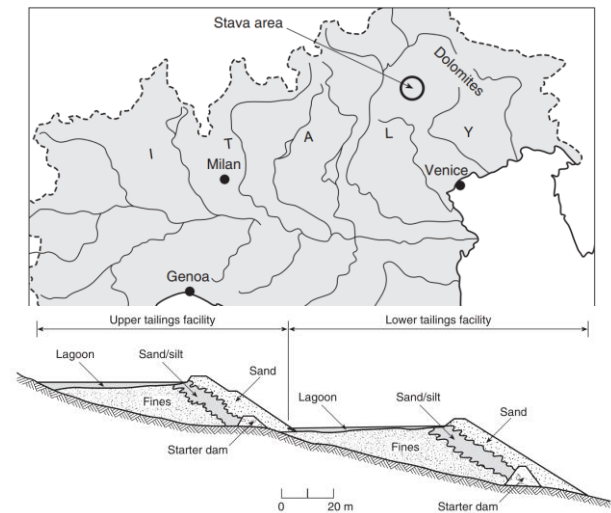


Fig. 2 Geographical localization of Stava village and schematic section of the two dams (Sarsby 2013)

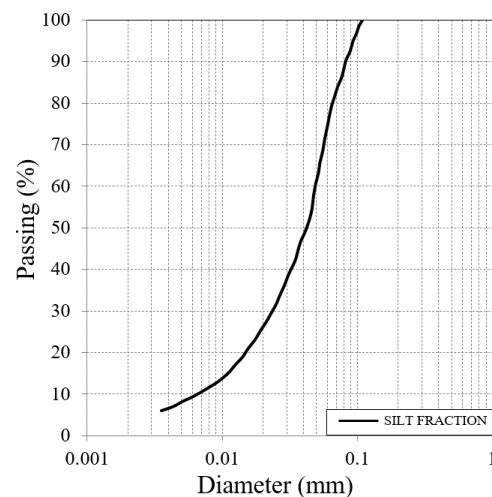


Fig. 3 Grain size distribution of the silt fraction of the Stava tailings (modified from Carrera *et al.* 2011)

The liquid limit is  $w_L=27.4\%$ , the plastic limit is  $w_P=18.0\%$  (plasticity index  $PI=9.4\%$ ) and the specific gravity  $G_s$  is 2.83. X-ray diffraction analysis showed that the silt fraction was made of quartz, with a significant amount of calcite and fluorite (Bella *et al.* 2017).

#### 3.2 Water retention behavior

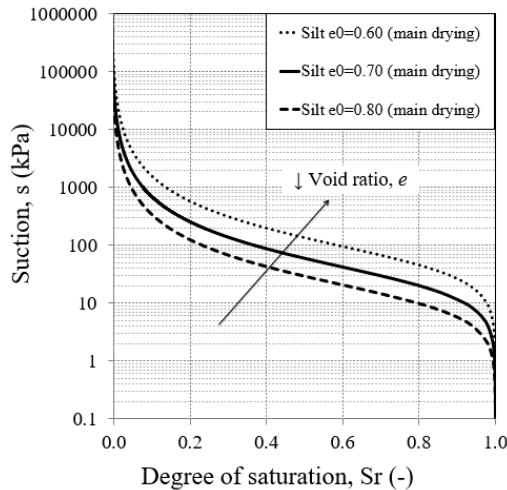
Previous studies (Bella *et al.* 2024, Bella and Musso 2022, Bella 2021) dealt with the characterization of the water retention behavior of the studied material. The retention properties were found to largely depend on the void ratio. Such a dependency was interpreted through the expression of Gallipoli *et al.* (2003)

$$S_r = \frac{1}{(1 + [\Phi(v-1)\psi_s]^n)^m} \quad (1)$$

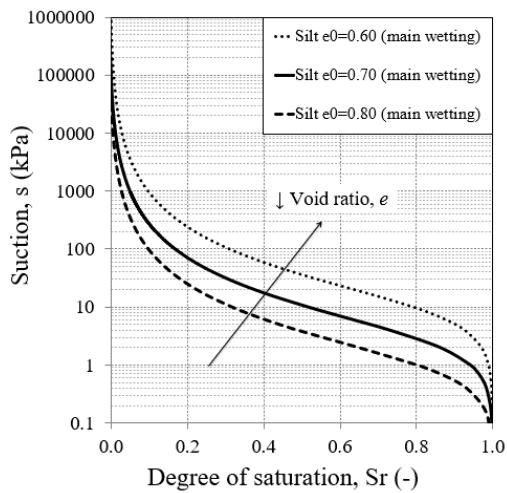
where  $v$  is the specific volume and  $n$ ,  $m$ ,  $\psi$ ,  $\Phi$  are soil model parameters summarized in Table 1.

Table 1 Parameters of the water retention model of Gallipoli *et al.* (2003) for the studied material (main drying branch and main wetting branch)

Main drying branch				Main wetting branch			
n	m	$\Phi$	$\Psi$	n	m	$\Phi$	$\Psi$
(-)	(-)	(kPa <sup>-1</sup> )	(-)	(-)	(-)	(kPa <sup>-1</sup> )	(-)
1.67	0.40	0.28	5.32	1.50	0.33	5.40	7.81



(a)



(b)

Fig. 4 Influence of void ratio on the water retention behavior of the Stava silty tailings: (a) main drying branch and (b) main wetting branch

The dependency of the main drying and main wetting curves on the void ratios of interest for this study are reported in Fig. 4.

#### 4. Methodology

The methodology adopted aimed at studying the mechanical response of the material upon undrained loading at relatively high degrees of saturation (nearly saturated conditions), by using a triaxial cell and imposing strain-controlled loading paths in undrained conditions.

#### 4.1 Sample preparation

Specimens initial sizes 38 mm diameter, and 76 mm height were created by imposing different initial values of void ratio and water content and using different preparation methods:

- the moist tamping technique (MT) was applied to compact samples TXT\_1-TXT\_6. This technique was adopted to obtain the same soil fabric and results comparable to those obtained by Carrera (2008, 2011), which were used as a reference for the saturated condition. According to Carrera (2008), the fabric created is likely to be similar to that of the moist, unsaturated materials that were placed in the Stava embankment. MT consists of creating five layers of a certain height and constant density inside the triaxial cell by manually compacting the wet material. Imposing the desired initial void ratio, total volume and water content, the total weight of the soil is obtained. The total weight is divided into five parts and each one will occupy 1/5th of the total volume, assuring that the density is homogeneous. The dry soil of each layer was mixed with 5% in weight of demineralized, de-aired water. The mixture corresponding to the first layer was then put into a split mold inside the triaxial cell and a tamper was adopted to gently compact the layer until it reached 1/5th of the total height. Some furrows were traced on the upper surface to obtain a better connection between the following layers. The procedure was then repeated until the last layer, reaching the total height of the sample;

- external compaction method (EC) was adopted to prepare samples TXT\_7-TXT\_8. The samples were prepared by hand-mixing a certain amount of dry soil with the required amount of demineralized, de-aired water to obtain an initial water content equal to 21.2%. The mixture was then put into a cylindrical mold, where it was statically compacted by means of three layers until it reached a total height of 76mm. The samples were then extracted from the mold and placed inside the triaxial cell. A value of  $w_0=21.2\%$  was the maximum initial water content to give a sample stiff enough to sustain itself once after its extraction from the mold and placement inside the cell.

The list of samples, their initial void ratio ( $e_0$ ), water content ( $w_0$ ), and dry weight ( $\gamma_d$ ) is given in Table 2.

#### 4.2 Experimental apparatus and testing phases

The hydro-mechanical behavior in nearly saturated conditions was investigated by means of monotonic triaxial tests. All the tests were carried out at Politecnico di Torino (Italy) by using a Bishop and Wesley's cell under displacement-controlled conditions. The cell allows independent control of the confining pressure and of the axial load and allows performing compression tests upon both loading and unloading paths. Thus, also along isotropic loading the piston was exerting a load on the sample, that was controlled independently from the radial stress. The apparatus was provided with a bottom and a top water drainage externally connected with two differential diaphragm pressure transducers (maximum pressure 1000 kPa; accuracy:  $\pm 0.5$  kPa) to record the pore water pressures.

Table 2 Initial state: preparation method, void ratio ( $e_0$ ), water content ( $w_0$ ), dry density ( $\gamma_d$ )

Sample	Preparation technique	$e_0$ (-)	$w_0$ (%)	$\gamma_d$ (kN/m <sup>3</sup> )
TXT_1	(MT)*	1.22	5.0	12.8
TXT_2	(MT)*	1.23	5.0	12.8
TXT_3	(MT)*	1.20	5.0	12.8
TXT_4	(MT)*	1.25	5.0	12.8
TXT_5	(MT)*	1.34	5.0	12.8
TXT_6	(MT)*	1.20	5.0	12.8
TXT_7	(EC)**	1.00	21.2	13.9
TXT_8	(EC)**	1.06	21.2	13.9

\* MT = sample compacted inside the triaxial cell with the moist tamping technique.

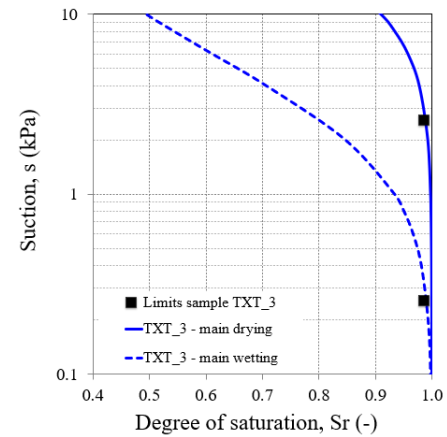
\*\* EC = sample externally compacted.

Two non-contact ‘Kaman’ sensors at opposite sides of the samples allowed measuring radial displacements. They were fixed on vertical bars placed in the cell chamber. The bars are connected to the bottom of the cell, and they can be moved radially by an external control so to allow proper measurements with the ‘Kaman’ throughout the duration of the test.

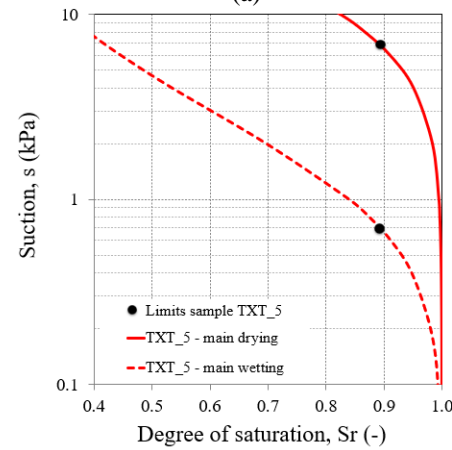
- the first step consisted of upward flushing with de-aired water, followed by back pressuring.
1. flushing of air bubbles was imposed by circulating de-aired water throughout the triaxial system (specimen, drainages, etc.) under a total confining stress equal to 10kPa. Flushing was realized by connecting sample drainages with a plastic box containing de-aired water. The container was placed at a certain height above the sample, to have a proper hydraulic head to allow the flushing of water within the sample in an upward direction. This step was also aimed to ensure that drainages were filled with water and represents a fundamental requirement for the following B-checking procedure. Flushing was usually not sufficient to obtain a high degree of saturation, so that was followed by a back-pressuring phase. In each test, flushing induced a volume reduction, due to a suction decrease. The volume strain was small (about 1%) for the externally compacted specimens, because of the high degree of saturation imparted at preparation. On the contrary, it was quite large (average value of 12%) for the moist tamped specimens, which were prepared at a low degree of saturation.
  2. Dissolution of a portion of the residual air inside the sample was obtained by the application of a backpressure, allowing to evaluate the -B Skempton parameter (wetting phase) according to the following expression

$$B = \Delta u_w / \Delta p \quad (2)$$

where  $\Delta u_w$  is the measured change in pore pressure and  $\Delta p$  is the imposed change in mean total stress. In the current research, each B-check phase induced a volume strain of approx. 3%. The values of B imposed in the tests ranged between 0.89-0.99. Most of these values are



(a)



(b)

Fig. 5 Water retention curves, degree of saturation, and suction limits at the end of consolidation: (a) sample TXT\_3 and (b) sample TXT\_5

below what is required for full saturation: this was chosen on purpose, so to deliberately have samples relatively close to saturation, but not fully saturated.

- Samples were then isotropically consolidated increasing simultaneously radial and axial stresses in drained conditions to achieve the desired effective stress (about 85 kPa). The consolidation phase was concluded when measures of the water volume change between the sample and volume meter showed no further variations.
- Finally, the shearing phase was carried out in undrained conditions at constant radial total stress under strain-controlled conditions by means of an axial force given by a piston connected to a digital pressure-volume controller (displacement rate=0.012 mm/min).
- At the end of the shearing phase, the water content was determined according to ASTM D2216 standard, by weighing the sample with a balance having accuracy +/- 0.0001g before and after drying in an oven at 105°C for 24 hours. According to the standard, this ensures an accuracy of 0.1%. The degree of saturation at the end of consolidation was determined by combining the water content with the void ratio at the end of consolidation, obtained on the basis of the corresponding volume strains (Table 3).

It is important to notice that the water ratio  $e_w$  (ratio between the volume of water and the volume of solids) increased during the flushing, the B-checks, and the consolidation stages. In general, samples explored a complex wetting process: during the flushing stage, wetting was caused by the entrance of water in the samples and also by the decrease in volume. During the 'B-checks' and the consolidation, wetting was caused by the decrease in the sample volume, not accompanied by an identical decrease in water volume. As the void ratio decreased during all of these stages, the position of the main branches of the water retention curves evolved as well, with a general increase in the air entry value and air occlusion values (see Fig. 5). For each test, the suction attained at the end of consolidation was unknown. However, it must lay within the range given by the suctions which, introduced in Eq. (1) together with the specific volume of the sample, predict the degree of saturation determined at the end of consolidation. By way of example, Fig. 5 provides the main branches of the water retention curves, the degree of saturation, and the limits of the admissible suction ranges for tests TXT\_3 and TXT\_5.

The admissible suction ranges thus determined for each test are provided in Table 3. It can be observed that they are generally smaller than the air entry values  $AEV=[\Phi(v-1)]^{-\psi}$  of the water retention characterization, suggesting that the samples might be in a state of *insular air saturation*, i.e. the air phase might not be continuous.

## 5. Experimental results and interpretation

In Section 5.1 the relationship between the -B value and the degree of saturation is shown for Stava tailings. After that, in Sections 5.2, 5.3, and 5.4 the investigation of the influence of the preparation technique, the water ratio, and void ratio on the hydro-mechanical behavior under unsaturated conditions is explored. Results are also compared with literature data obtained on tailings or other inert soils. The dependency of the static liquefaction susceptibility on the degree of saturation and excess of pore pressure is investigated in section 5.5. Finally, a preliminary interpretation of the static liquefaction response under saturated and unsaturated conditions is given in section 5.6 on the basis of the relationship between degree of saturation and suction (Water Retention Curve) within the Critical State theory.

### 5.1 Relationship between the -B value and the degree of saturation

The analysis of the relationship between the degree of saturation and the -B values determined during the preliminary stages of the tests further confirms the state of *insular air saturation*. When an unsaturated soil is loaded in undrained conditions, the water pressure and the air pressure generally increase by a different amount. Therefore, two different pore pressure coefficients  $B_a$  and  $B_w$  can be defined, one for each fluid. At high degrees of saturation, when the air phase is not continuous,  $B_a$  and  $B_w$  converge to an identical value -B (see e.g., Fredlund *et al.*

2012). This can be explained by the insular condition of air into the water phase when the degree of saturation is high. For soil composed of incompressible grains and saturated with a compressible fluid, Skempton's -B parameter is given by

$$B = K_f / [K_f + nK] \quad (3)$$

where  $K_f$  is the bulk modulus of the fluid,  $K$  is the bulk modulus of the solid skeleton and  $n$  is porosity. The overall compressibility of a mixture of fluids, where one is 'entrapped' in the other, can be determined according to the Reuss lower bound (Mavko *et al.* 2009) as the sum of the compressibility of its constituents weighed by their volume fraction. Thus, for the air and the water in the pores, it follows

$$1/K_f = S_r/K_w + [(1 - S_r)/K_a] \quad (4)$$

where  $K_w$  is the bulk modulus of water (2.2 GPa) and  $K_a$  is the bulk modulus of air. By treating air as an ideal gas it follows  $K_a = 1/u_a^*$ , where  $u_a^*$  is the absolute value of the air pressure, i.e.,  $u_a^* = u_a + u_{atm}$ ,  $u_{atm}$  being the atmospheric pressure. As the suction in the tests was quite small, it was also assumed that  $u_a \cong u_w$ . If Eq. (4) is introduced into Eq. (3), the B-value can be expressed as a function of the degree of saturation

$$B_R = \frac{\frac{K_w K_a}{(1 - S_r)K_w + S_r K_a}}{\frac{K_w K_a}{(1 - S_r)K_w + S_r K_a} + \left(\frac{e}{1 + e}\right)K} \quad (5)$$

The bulk modulus  $K$  of Stava silty tailing was obtained as the ratio between the increase in mean effective stress  $\Delta p'$  and in volumetric strain  $\Delta \varepsilon_v$  during the consolidation phase. The former was assumed to be equal to Terzaghi's in these high saturation conditions

$$K = (\Delta p - \Delta u_w) / \Delta \varepsilon_v \quad (6)$$

The measured -B values and degree of saturation (solid points) are plotted into the (B-Sr) plane with the theoretical value for the lower Reuss bound (Eq. (5)), as shown in Fig. 6. All the points are quite close to the lower Reuss bound, confirming the state of air insular saturation in the tests.

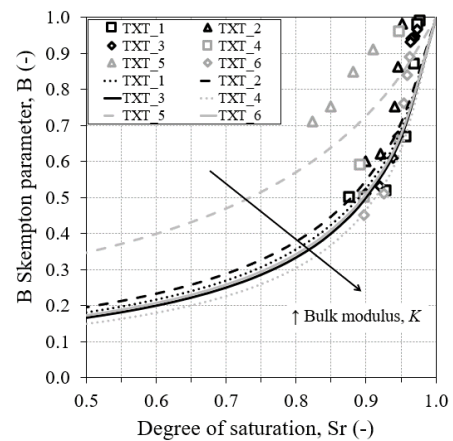


Fig. 6 Relationship between -B value and  $S_r$ : Reuss lower bound (lines) and experimental points TXT\_1→TXT\_6

Table 3 State of the samples at the end of the consolidation phase: void ratio ( $e_c$ ), degree of saturation ( $S_r$ ), maximum and minimum suction ( $s_c$ ), water ratio ( $e_w$ ) and comments

Sample	Void ratio $e_c$ (-)	Degree of saturation $S_r$ (-)	Max. suction $s_c$ (kPa)	Min. suction $s_c$ (kPa)	Water ratio $e_w$ (-)	Comments
TXT_1	0.82	0.98	1.5	0.15	0.80	Liquefied
TXT_2	0.84	0.97	2.0	0.15	0.82	Liquefied
TXT_3	0.71	0.98	4.0	0.40	0.70	Liquefied
TXT_4	0.82	0.94	3.5	0.30	0.77	Liquefied
TXT_5	0.78	0.89	8.5	0.85	0.69	Not liquefied
TXT_6	0.75	0.97	3.0	0.30	0.73	Liquefied
TXT_7	0.90	0.96	1.5	0.15	0.86	Not liquefied
TXT_8	1.00	1.00	$\approx 0$	$\approx 0$	1.00	Not liquefied

## 5.2 Influence of the preparation technique

The effect of the preparation technique on the hydro-mechanical behavior of specimens of Stava tailings is investigated. The stress paths of three samples are shown in Fig. 7.

The samples were prepared by means of the moist tamping method (TXT\_4) and external compaction procedure (TXT\_7, TXT\_8). Despite their degree of saturation being similar at the end of the consolidation (Table 3), they exhibited different stress-strain responses. Indeed, the looser specimens TXT\_7 and TXT\_8 showed a hardening behavior, while test TXT\_4, even if denser, approached the Steady State by means of a softening response. This difference can be appreciated in terms of excess of pore pressure developed during the undrained shearing phase. The excess of pore pressure of sample TXT\_4 reached a value  $\Delta u_w = 78$  kPa and then it remained constant. The stress path of sample TXT\_4, plotted in terms of  $p-u_w$ , allows to identify the Instability Line (Fig. 7(a)). On the contrary, the excess of pore pressure of samples TXT\_7 and TXT\_8 reached a peak value  $\Delta u_w = 60$  kPa and then decreased. Such a response is a consequence of the transitional behavior of these samples which, at large axial strains, exhibited a stress-hardening behavior (Fig. 7(b)). During these tests, the stress ratio shifted toward the Critical State Line (CSL), and no liquefaction susceptibility was observed.

These outcomes can be well compared with the literature results obtained by Chu *et al.* (2003) on sandy gold tailings. The Authors performed two undrained triaxial tests on two specimens prepared by the moist tamping technique (MT) and the water sedimentation method (WS). Both specimens were consolidated under the same effective confining stress ( $p'_c = 150$  kPa) and the void ratios after consolidation were about the same. Still, softening only occurred for the MT specimen and not for the one prepared by using the water sedimentation method. Also in this case the variations in stress-strain behavior are supposed due to the different soil fabric (particle arrangement) created by using different techniques. The importance of the preparation method on the stress-strain response of tailings is also given by analyzing the outcomes obtained by Correa and Filho (2019). The Authors performed some triaxial tests on saturated silty-sandy tailings collected at a mine site in

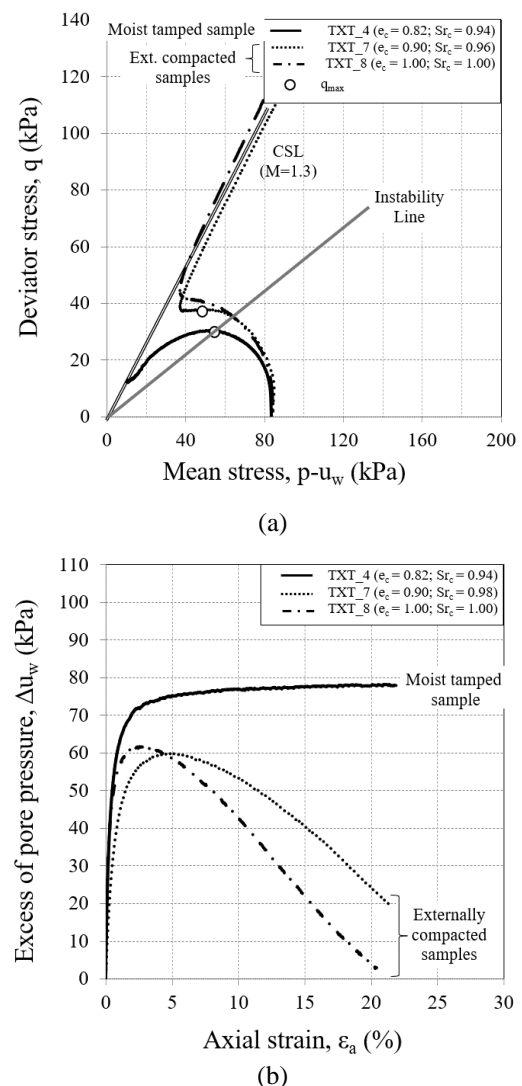


Fig. 7 Effect of the preparation technique on the hydro-mechanical behavior of Stava tailings: (a) stress paths and (b) excess of pore pressure with axial strain

the Quadrilatero Ferrifero (Minas Gerais, Brazil) and prepared by the moist tamping and the slurry deposition method. All the specimens were consolidated under the same effective confining stress and the density after consolidation was similar. The two preparation techniques

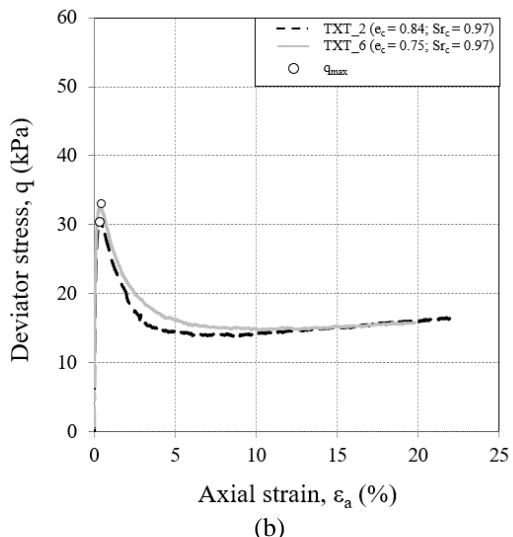
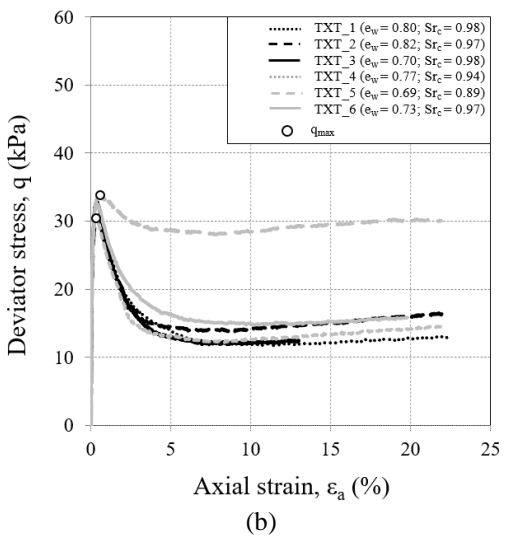
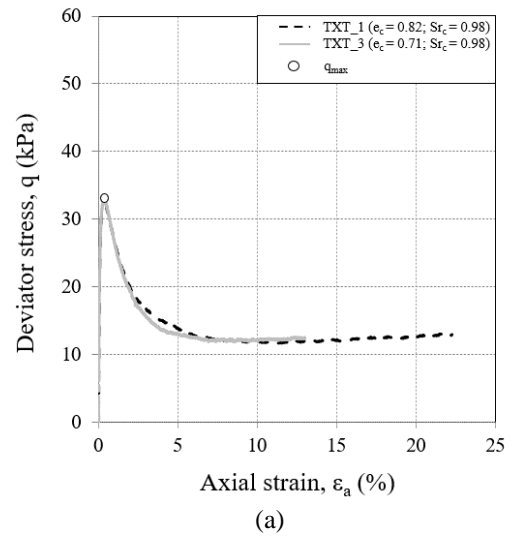
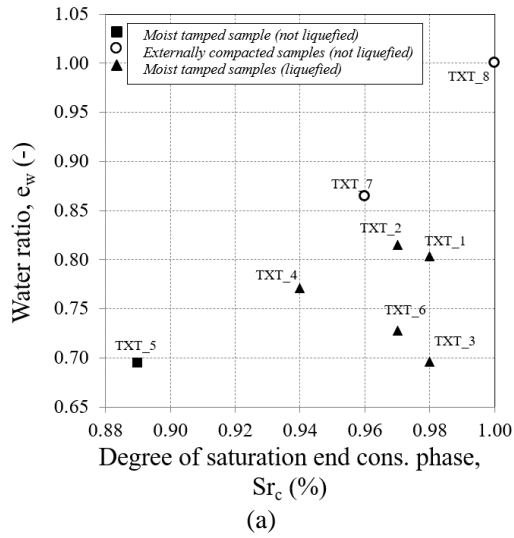


Fig. 8 Relationship between water ratio and degree of saturation: (a)  $e_w$ - $Sr_c$  plane and (b) stress-strain curves of the MT Stava specimen

Fig. 9 Effect of void ratio on the stress-strain curves of moist tamped Stava specimen

allowed to obtain different patterns, indeed the moist tamped samples showed to be more prone to liquefy than the specimen created by the slurry deposition technique.

### 5.3 Influence of water ratio

The water ratio  $e_w$  at the end of each consolidation phase was evaluated as (Table 3)

$$e_w = Sr_c \cdot e_c \quad (7)$$

where  $Sr_c$  and  $e_c$  are the degree of saturation and void ratio at the end of the consolidation phase, respectively. Test TXT\_5 has the lowest water ratio ( $e_w=0.69$ ) if compared to the others, respectively TXT\_1 ( $e_w =0.80$ ), TXT\_2 ( $e_w =0.82$ ), TXT\_3 ( $e_w =0.70$ ), TXT\_4 ( $e_w =0.77$ ) and TXT\_6 ( $e_w =0.73$ ), as shown in Fig. 8.

Within the investigated range of void ratios and degrees of saturation, results suggest that no significant effects of water ratio on the static liquefaction susceptibility can be easily appreciated.

### 5.4 Influence of void ratio

The effect of the initial density on the stress-strain response of Stava tailings was investigated. As shown in Fig. 9(a), samples TXT\_1 and TXT\_3 were prepared by the same technique (MT) and both had a  $Sr_c=0.98$ , but their void ratios at the end of the consolidation phase were different because of the different volumetric strains that occurred during the flushing stage ( $e_c=0.82$  for TXT\_1 and  $e_c=0.71$  for TXT\_3). Despite this difference, they showed the same response when sheared. A very similar response was observed also for samples TXT\_2 and TXT\_6 (Fig. 9(b)), which also had different initial densities but the same degree of saturation. It might therefore be concluded that, over the range of degrees of saturation and void ratio explored, the value of the void ratio had a negligible effect on the deformation behavior.

### 5.5 Influence of the degree of saturation and role of the excess of pore pressure

The effect of the degree of saturation on the hydraulic and

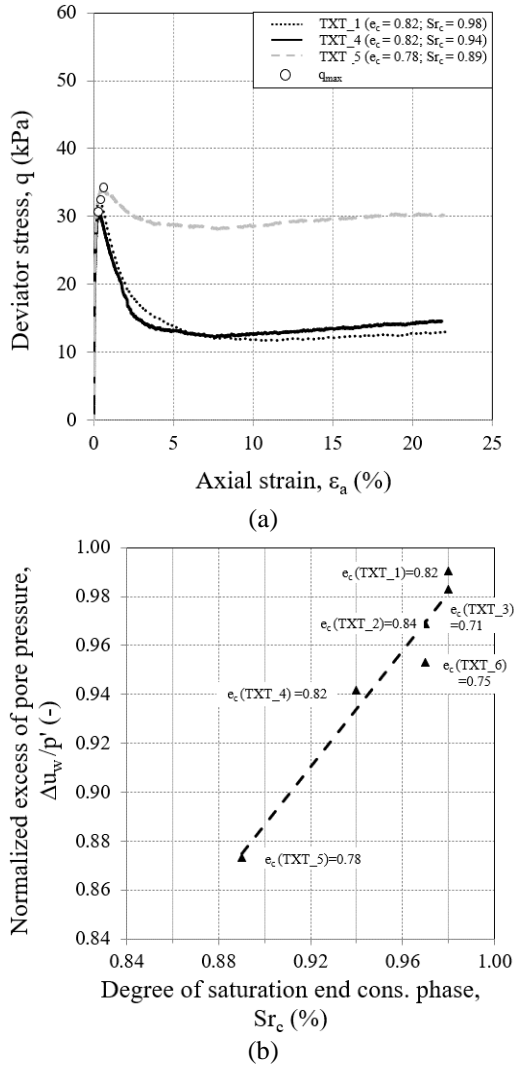


Fig. 10 (a) Effect of the degree of saturation on the stress-strain curves of moist tamped Stava specimen and (b) normalized excess of pore pressure

mechanical behavior of tailings was studied for MT samples. The void ratio at the end of the consolidation phase for tests TXT\_1, TXT\_4, and TXT\_5 was similar, but their degree of saturation was different ( $e_c = 0.82$  and  $Sr_c = 0.98$  for TXT\_1;  $e_c = 0.82$  and  $Sr_c = 0.94$  for TXT\_4;  $e_c = 0.78$  and  $Sr_c = 0.89$  for TXT\_5;) as shown in Fig. 10(a). Sample TXT\_5 showed a maximum deviator stress ( $q_{max} = 34$  kPa at  $\varepsilon_a = 0.6\%$ ), higher than those experimented by sample TXT\_4 ( $q_{max} = 30$  kPa at  $\varepsilon_a = 0.20\%$ ) or sample TXT\_1 ( $q_{max} = 32$  kPa at  $\varepsilon_a = 0.30\%$ ). The residual value of the deviator stress of sample TXT\_5 was 30 kPa, twice the one of test TXT\_4 and TXT\_1. These results seem to suggest that, in the context of the Stava tailings, a degree of saturation below about 0.90 is sufficient to significantly reduce the softening. These results are in good agreement with the experimental outcomes obtained from soils sheared by carrying out monotonic and cyclic tests (Vernay *et al.* 2018, Vernay *et al.* 2017, Arab *et al.* 2015). If the maximum excess of pore pressure developed during the undrained shearing phase of each test is divided by the

effective mean stress, the evolution of the ratio  $\Delta u_w/p'$  with the degree of saturation can be observed, as shown in Fig. 10(b).

A contractive behavior at high degree of saturation state was expected but, because of the undrained conditions, saturated samples (TXT\_1  $\rightarrow$  TXT\_4 and TXT\_6) were not allowed to contract, leading the pore pressure to increase, leading to loss of the shear strength. On the other side, when the degree of saturation of the unsaturated sample is below 0.90 (TXT\_5) the developed excess of pore pressure is much less than that of saturated samples, leading to a higher strength also for loose sample that could be prone to liquefy because of their initial density. This response appears to be linked to the higher amount of air, which in light of Eq. (4) increases the compressibility of the air-water system, even in nearly saturated conditions.

### 5.6 A preliminary interpretation of the static liquefaction response of Stava tailings within the Critical State Framework

The Critical State is a condition in which, as deformations proceed with shearing, a volume of soil tends toward an ultimate state in which shearing strains can continue without further variations of volumetric strain, deviatoric stress, or mean effective stress. In unsaturated conditions, no variations of water ratio are also expected with shearing strain, so that

$$\frac{\partial \varepsilon_v}{\partial \varepsilon_s} = \frac{\partial q}{\partial \varepsilon_s} = \frac{\partial p'_B}{\partial \varepsilon_s} = \frac{\partial e_w}{\partial \varepsilon_s} = 0 \quad (8)$$

where  $\varepsilon_v$  is the volumetric strain,  $\varepsilon_s$  is the deviatoric strain,  $q$  is the deviatoric stress,  $p'_B$  is the mean effective stress (e.g., according to the Bishop definition  $p'_B = p_{net} + \chi \cdot s$ , assuming  $\chi = Sr$  and  $p_{net}$  as the difference between average tension and air pressure) and  $e_w$  is the water ratio. Within the framework of the Critical State, the susceptibility of a granular soil to liquefy is related to the state parameter (Been and Jefferies 1985)

$$\psi = e - e_{cs} \quad (9)$$

where  $e$  is the void ratio, while  $e_{cs}$  is the void ratio at Critical State under the same mean stress. A positive value of the state parameter is related to loose specimens prone to liquefy, whereas a negative value of the state parameter is related to dense specimens with a dilatative behavior. The Critical State Line derived from the final conditions of triaxial tests performed by Carrera (2008) on saturated Stava tailings is plotted in Fig. 11(a) (solid line). In the same figure, the Critical State Lines associated with unsaturated samples tested in another experimental campaign by means of suction-controlled triaxial tests (Bella 2017, Bella and Musso 2023) are also provided. Those are expressed in terms of mean Bishop effective stress  $p'_B$  ( $p'_B = p - Sr \cdot s$ ) and were found to depend on suction: the figure provides the ones for  $s = 30$  kPa and  $s = 45$  kPa. In the same compression plane, the initial state of Stava MT samples is given by the red symbols. Their suction can be estimated with the procedure described in Section 5. In general and for all samples, this estimates

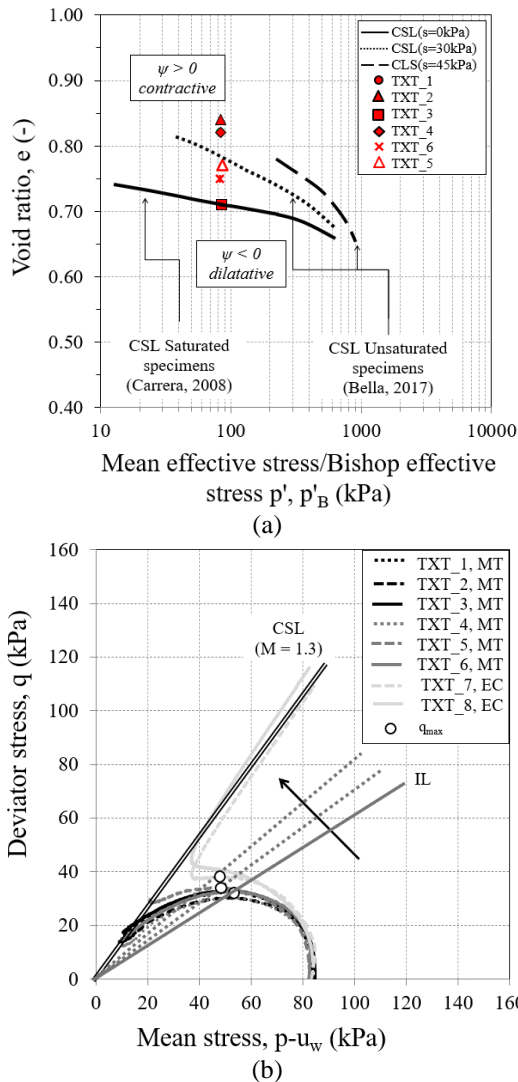


Fig. 11 (a) CSL for saturated (solid line) and nearly saturated specimens (dotted lines) and initial state of nearly saturated Stava tailings (red symbols) and (b) Critical State Line, Instability Line, stress paths and locus of  $q_{max}$  (modified from Bella 2017)

ranges between 0.15 and 4 kPa with a higher range for sample TXT\_5 ( $0.85 \text{ kPa} < s < 8.5 \text{ kPa}$ ). Considering the constant water volume imposed by the undrained condition, during the test suction should then remain grossly within this range. With reference to its initial state in the compression plane (Fig. 11(a)), the empty triangle should be associated with an unsaturated Critical State Line well below  $CSL:s=30 \text{ kPa}$  and close to the one of the saturated state. Therefore, in principle, TXT\_5 has a positive state parameter, but liquefaction cannot take place since the pore pressure increase during shearing was rather small (Fig. 10(a)). This can be explained considering that as the degree of saturation decreases the induced overpressure decreases as well, as also detected for the  $-B$  parameter. On the other hand, the pore pressure increase developed during tests TXT\_1→TXT\_4 and TXT\_6 was large enough to bring these samples to liquefaction, as confirmed by the experimental results in Figs. 9 and 10. This larger pore

pressure increase can also be explained in terms of the reduced compressibility of the pore fluid mixture and by the evolution of  $-B$  parameter with the degree of saturation. The stress paths of the unsaturated Stava tailings are represented in Fig. 11(b).

The transitional behavior of TXT\_7 and TXT\_8 can be easily identified. On the other side, all the other nearly saturated samples prepared by the moist tamped method exhibited a contractive behavior. The Instability Line (IL) is also identified as the solid line passing through the peak deviator stresses of liquefied samples. These outcomes are consistent with Carrera (2008), who suggested that samples showing a peak deviator stress  $q_{max}$  between the CSL and the IL were less prone to liquefy. The projection of the Critical State Line in the  $(p',q)$  has slope  $M=1.3$  in good accordance with Carrera (2008) for fully saturated conditions.

## 6. Conclusions

Static liquefaction has been widely recognized as one of the major causes of tailing dams collapse, causing the loss of lives and severe environmental and economic impacts. Tailing dams interact with the atmosphere, and their shallower parts tend to be unsaturated.

In order to account for the possibility of static liquefaction also in unsaturated conditions, analyses should be able to reproduce the pore water pressure and degree of saturation in the vadose zone. This implies a preliminary characterization of the water retention properties of the material and an adequate knowledge of the interaction of the shallower surface layers with the atmosphere.

This research presented a preliminary insight into the hydro-mechanical behavior of the Stava silty tailings in nearly saturated conditions, and a relationship between the Skempton's  $-B$  parameter and the degree of saturation is given. The effects of the preparation technique, the water ratio, void ratio, and the degree of saturation on the static liquefaction response were investigated and compared with the experimental results on other tailings or inert soils.

- The influence of the preparation technique was first investigated by comparing the stress-strain response of moist tamped samples with other samples prepared by using an external compaction procedure. This condition might represent different deposition methods of tailings inside the basin. While EC samples did not have any tendency to liquefy, MT samples tended towards liquefaction even when shearing started from void and water ratios lower than those of the EC samples. The experimental results were in good agreement with literature data obtained on fully saturated sandy-silty tailings, deducing that the preparation method strongly affects the mechanical behavior since it leads to a different soil fabric.
- Samples with the same degree of saturation but different densities were tested. Within the degree of saturation and void ratios investigated, all of the latter resting above the projection on the compression plane of the Critical State Line, the increase of density had no relevant effects on the mechanical behavior of Stava tailings.

- The pore pressure increments developed during the shearing phases were strictly related to the sample's degree of saturation. Smaller degrees of saturation lead to smaller overpressures: in the explored range ( $S_r > 0.89$ ) the relationship between them was found to be about linear.
- Since the overpressure decreases as the degree of saturation decreases, the tendency to liquefy also decreases. In the MT experiments, softening almost didn't occur for the sample with a degree of saturation of about 0.90, while it always occurred at higher degrees of saturation. For soil in a state of air insular saturation, such as the cases explored in this study, this degree of saturation might be a limit below which liquefaction does not occur.

## Acknowledgments

The Authors wish to thank Dr. A. Azizi, Dr. O. Pallara, and Mr. G. Bianchi (Politecnico di Torino) for their help during the laboratory tests presented in this work.

## References

- Abdallah, K., Abdelkader, B., Ahmed, A., Eddine, B.D. and Marwan, S. (2021), "A laboratory study of shear strength of partially saturated sandy soil", *Geomech. Geoeng.*, 1-10. <https://doi.org/10.1080/17486025.2020.1864034>.
- Alonso, E.E. and Gens, A. (2006), "Azna collar dam failure. Part1: Field observations and material properties", *Geotechnique*, **56**(3), 165-183. <https://doi.org/10.1680/geot.2006.56.3.165>.
- Arab, A., Belkhatir M. and Sadek, M. (2015), "Saturation effect on behaviour of sandy soil under monotonic and cyclic loading: A laboratory investigation", *Geotech. Geol. Eng.*, **34**(1), 347-358. <https://doi.org/10.1007/s10706-015-9949-6>.
- ASTM D2216-19 Standard test methods for laboratory determination of water (Moisture) content of soil and rock by mass.
- Becker, L.D.B., Ehrlich, M. and Barbosa, M.C. (2023), "Discussion of "Stability Analysis of Upstream Tailings Dam Using Numerical Limit Analyses", *J. Geotech. Geoenviron. Eng.*, **149**(3). <https://doi.org/10.1061/JGGEFK.GTENG-11272>.
- Been, K. and Jefferies, M. (1985), "A state parameter for sands". *Geotechnique*, **35**(2), 99-112. <https://doi.org/10.1680/geot.1985.35.2.99>.
- Bella, G. (2017), "Hydro-Mechanical behaviour of tailings in unsaturated conditions", Ph.D. Dissertation, Politecnico di Torino, Torino.
- Bella, G. (2021), "Water retention behaviour of tailings in unsaturated conditions", *Geomech. Eng.*, **26**(2), 117-132. <https://doi.org/10.12989/gae.2021.26.2.117>.
- Bella, G. and Musso, G. (2022), "Water retention response of unsaturated Stava tailings", *Proceedings of the 8th International Conference on Tailings Management (TAILINGS 2022)*, Hugo Quelopana, 6/8 of July, 2022.
- Bella, G., Lameiras, F., Esposito, T., Barbero, M. and Barpi, F. (2017), "Aging simulation of the tailings from stava fluorite extraction by exposure to gamma rays", *Revista Escola de Minas*, **70**(4). <https://doi.org/10.1590/0370-44672016700-163>.
- Bella, G., Ghezzi, S., Czarski, D., Ambrosi, C., Lüscher, M. and Giani, M. (2024), "Preliminary evaluation of the effects of the unsaturated conditions on the compressibility and pre-shearing state of stress of quartzitic tailings", *Proceedings of the 9th International Conference on Geotechnical Research and Engineering (ICGRE 2024)*, Avestia Publishing, 14/16 of April 2024, London, UK. <https://doi.org/10.11159/icgre24.121>.
- Bella, G. and Musso, G. (2023), "Hydro-mechanical behaviour and Critical State Conditions of unsaturated silty tailings", *Proceedings of the 8th International Conference on Geotechnical Research and Engineering (ICGRE 2023)*, Avestia Publishing, 29/31 of March 2023, Lisbona, Portugal. <https://doi.org/10.11159/icgre23.114>.
- Bhanbhro, R. (2014), "Mechanical properties of tailings - basic description of a tailings material from Sweden", Ph.D. Dissertation, Luleå University of Technology, Sweden.
- Bishop, A.W. (1973), "The influence of an undrained change in stress on the pore-pressure in porous media of low compressibility", *Geotechnique*, **23**(3), 435-442. <https://doi.org/10.1680/geot.1973.23.3.435>.
- Carmo, F.F., Kamino, L., Juniora, R., de Camosa, C., do Carmo, F., Silvino, G., de Castro, K., Mauro, M., Rodrigues, N., Miranda, M. and Pinto C. (2017), "Fundão tailings dam failures: the environment tragedy of the largest technological disaster of Brazilian mining in global context", *Perspect. Ecol. Conserv.*, **15**(3), 145-151. <https://doi.org/10.1016/j.pecon.2017.06.002>.
- Carrera, A. (2008), "Mechanical behaviour of Stava tailings", Ph.D. Dissertation, Politecnico di Torino, Torino.
- Carrera, A., Coop, M. and Lancellotta, R. (2011), "Influence of grading on the mechanical behaviour of Stava tailings", *Geotechnique*, **61**(11), 935-946. <https://doi.org/10.1680/geot.9.P.009>.
- Chu J., Leong, W.K. and Loke, W.L. (2003), "Discussion of "defining an appropriate steady state line for Marriespruit gold tailings", *Can. Geotech. J.*, **40**(2), 484-486. <https://doi.org/10.1139/t02-118>.
- Carrier, W.D. (1991), "La ingegneria Geotecnica nella Salvaguardia e Recupero del Territorio", *Proceedings of the 15th Conference of Geotechnics of Turin (XV CGT)*, 20/22 November, 1991, Torino, Italy.
- Correa, M.M. and Filho, W.O. (2019), "Impact of methods used to reconstitute tailing specimens on the liquefaction potential assessment of tailing dams", *Revista Escola de Minas*, **72**(3). <https://doi.org/10.1590/0370-44672018720164>.
- Daouadji, A., AlGali, H., Darve, F. and Zeghloul, A. (2010). "Instability of granular materials: Experimental evidence of diffuse mode of failure for loose sands", *J. Eng. Mech.*, **136**(5), 575-588. [https://doi.org/10.1061/\(ASCE\)EM.1943-7889.0000101](https://doi.org/10.1061/(ASCE)EM.1943-7889.0000101).
- Davies, M., Martin, T. and Lighthall, P. (2000), "Mine Tailing Dams: When Things Go Wrong". *Proceedings of the Tailing Dams 2000*, Association of State Dam Safety Officials, U.S. Committee on Large Dams, Las Vegas, Nevada. <http://www.infomine.com/publications/docs/Davies2002d.pdf>.
- Deng, D., Wen, S., Lu, K. and Li, L. (2020) "Calculation model for the shear strength of unsaturated soil under nonlinear strength theory", *Geomech. Eng.*, **21**(3), 247-258. <https://doi.org/10.12989/gae.2020.21.3.247>.
- Flora, A., Bilotta, E., Lirer, S., Mele, L. and Modoni, G. (2023), "Liquefaction mechanism and mitigation techniques", *Italian Geotech. J.*, **2**, 33-88. <https://doi.org/10.19199/2023.2.0557-1405.033>.
- Fredlund, D.G., Rahardjo, H. and Fredlund, M.D. (2012), *Unsaturated soil mechanics in Engineering Practice*. John Wiley and Sons. [https://doi.org/10.1061/\(ASCE\)1090-0241\(2006\)132:3\(286\)](https://doi.org/10.1061/(ASCE)1090-0241(2006)132:3(286)).
- Gajo, A., Piffer, L. and de Polo, F. (2000), "Analysis of certain factors affecting the unstable behaviour of saturated loose sand", *Mech. Cohesive-Frictional Mater.*, **5**(3), 215-237.
- Gallipoli, D., Wheeler, S.J. and Karstunen, M. (2003), "Modelling the variation of degree of saturation in a deformable unsaturated soil", *Geotechnique*, **53**(1), 105-112.

- <https://doi.org/10.1680/geot.2003.53.1.105>.
- Girardi, V. and Bella, G. (2023), "Application of the Material Point Method to the study of tailing dams failure due to static liquefaction", *Proceedings of the 8th Convegno Nazionale dei Ricercatori di Ingegneria Geotecnica (CNRIG 2023)*, Associazione Geotecnica Italiana Publishing, 05/07 of July 2023, Palermo, Italy. [https://doi.org/10.1007/978-3-031-34761-0\\_53](https://doi.org/10.1007/978-3-031-34761-0_53).
- Horn-Da, L., Chien-Chih, W. and Xu-Hui, W. (2018), "A simplified method to estimate the total cohesion of unsaturated soil using an UC test", *Geomech. Eng.*, **16**(6), 599-608. <https://doi.org/10.12989/gae.2018.16.6.599>.
- Leong, W.K., Chu, J. and Teh, C.I. (2000). "Liquefaction and instability of a granular fill material", *Geotech. Test. J.*, **23**(2), 178-192. <https://doi.org/10.1520/GTJ11042J>.
- Lucchi, G. (2015), "Genesi, cause e responsabilità della catastrofe del 19 luglio 1985 in val di Stava", *Proceedings of the "La sicurezza dei riempimenti di terra: bacini di decantazione, colmate e discariche"*, 15-19 of July, Stava, Italy.
- Lucchi, G. (2020), "Tailing Dams: lezioni dal passato e dal presente. Stava: cause e responsabilità", *Online Conference, GEAM*.
- Marabet, K., Benessalah, I., Chemmam, M. and Arab, A. (2019), "Laboratory study of shear strength response of Chlef natural sand: effect of saturation", *Marine Georesour. Geotec.*, **38**(1), 1-7. <https://doi.org/10.1080/1064119X.2019.1595792>.
- Mavko, G., Mukerji, T. and Dvorkin, J. (2009), "The rock physics handbook", Cambridge University Press.
- Mele, L., Chiaradonna, A., Lirer, S. and Flora, A. (2021), "A robust empirical model to estimate earthquake-induced excess pore water pressure in saturated and non-saturated soils", *Bull. Earthq. Eng.*, **19**(10), 3865-3829. <https://doi.org/10.1007/s10518-020-00970-5>.
- Mele, L. and Flora, A. (2019a), "On the prediction of liquefaction resistance of unsaturated sands", *Soil Dyn. Earthq. Eng.*, **125**, 1-12. <https://doi.org/10.1016/j.soildyn.2019.05.028>.
- Mele, L., Tan Tian, J., Lirer, S., Flora, A. and Koseki, J. (2019b), "Liquefaction resistance of unsaturated sands: experimental evidence and theoretical interpretation", *Geotechnique*, **69**(6), 541-553. <https://doi.org/10.1680/jgeot.18.P.042>.
- Morgenstern, N.R., Steven, G.V., Cássio, B.V. and Bryan, D.W. (2016), "Fundao tailings dam review panel – report on the immediate causes of the failure of the Fundao Dam", *Panel Report - 25 August, 2016*.
- Nagao, K., Suemasa, N., Jinguuji, M. and Nakazawa, H. (2015), "In-situ applicability test of soil improvement for housing sites using Micro-Bubbles against soil liquefaction in URAYASU", *Proceedings of the 25th international ocean and polar engineering conference*, 21/26 June 2015, Kona, Hawaii, USA.
- Olson, S.M., Stark, T.D., Walton, W.H. and Castro, G. (2000), "1907 Static liquefaction flow failure of the North Dike of Wachusett Dam", *J. Geotech. Geoenviron. Eng.*, **126**(12), 1184-1193. [https://doi.org/10.1061/\(ASCE\)10-90-0241\(2000\)126:12\(1184\)](https://doi.org/10.1061/(ASCE)10-90-0241(2000)126:12(1184)).
- Okamura, M., Takebayashi, M., Nishida, K., Fujii, N., Jinguuji, M., Imasato, T., Yasuhara, H. and Nakagawa, E. (2010), "In-Situ desaturation test by air injection and its evaluation through field monitoring and multiphase flow simulation", *J. Geotech. Geoenviron. Eng.*, **137**(7), 643-652. [https://doi.org/10.1061/\(ASCE\)GT.1943-5606.0000483](https://doi.org/10.1061/(ASCE)GT.1943-5606.0000483).
- Okamura, M. and Soga, Y. (2006), "Effects of pore fluid compressibility on liquefaction resistance of partially saturated sand", *Soils Found.*, **46**(5), 695-700. <https://doi.org/10.3208/sandf.46.695>.
- Pirulli, M., Barbero, M., Marchelli, M. and Scavia, C. (2017), "The failure of the Stava Valley tailings dams (Northern Italy): numerical analysis of the flow dynamics and rheological properties". *Geoenviron. Disasters*, **4**(3), 1-15. <https://doi.org/10.1186/s40677-016-0066-5>.
- Reuss, A. (1929), "Berechnung der Fließgrenze von Mischkristallen auf Grund der Plastizitätsbedingung für Einkristalle. Z. Angew.", *Math. Mech.*, **9**, 49-58.
- Rico, M., Benito, G., Salgueiro, A.R., Diez-Herrero, A. and Pereira H.G. (2008), "Reporting tailings dam failure – A review of the European incidents in the worldwide context", *J. Hazardous Mater.*, **152**(2), 846-852. <https://doi.org/10.1016/j.jhazmat.2007.07.050>.
- Sarsby, R. (2013), *Environmental Geotechnics*, ICE Publishing.
- Tran, K.H., Imazadeh, S., Said Taibi, Hanene Souli, Jean-Marie Fleureau and Mahdia Hattab (2023), "Liquefaction of unsaturated soils- volume change and residual shear strength", *Eur. J. Environ. Civil Eng.*, **27**(3), 1144-1164. <https://doi.org/10.1080/19648189.2022.2075471>.
- Tsukamoto, Y. (2019), "Degree of saturation affecting liquefaction resistance and undrained shear strength of silty sands", *Soil Dyn. Earthq. Eng.*, **124**, 365-373. <https://doi.org/10.1016/j.soildyn.2018.04.041>.
- Tsukamoto, Y., Kawabe, S., Matsumoto, J. and Hagiwara, S. (2014), "Cyclic resistance of two unsaturated silty sands against soil liquefaction", *Soils Found.*, **54**(6), 1094-103. <https://doi.org/10.1016/j.sandf.2014.11.005>.
- Unno, T., Kazama, M., Uzoka, R. and Sento, N. (2008), "Liquefaction of unsaturated sand considering the pore air pressure and volume compressibility of the soil particle skeleton", *Soils Found.*, **48**(1), 87-99. <https://doi.org/10.3208/sandf.48.87>.
- Unno, T., Kazama, M., Sento, N. and Uzuoka, R. (2006), "Cyclic shear behavior of unsaturated volcanic sandy soil under various suction conditions", *Geotech. Special Publication*, **147**(1), 1133.
- Vernay, M., Morvan, M. and Breul, P. (2018), "Influence of saturation degree on soil behavior toward liquefaction", *Proceedings of the 7th International Conference on Unsaturated Soils*, 03/05 of August 2018, Hong Kong.
- Vernay, M., Morvan, M. and Breul, P. (2017), "Influence of saturation degree on soil liquefaction behavior", *Proceedings of the 3rd International Conference on Performance-based Design in Earthquake Geotechnical Engineering (PBD-III)*, 16/19 of July 2017, Vancouver, Canada.
- Wanatowski, D. and Chu, J. (2007). "Static liquefaction of sand in plane strain", *Can. Geotech. J.*, **44**(3), 299-313. <https://doi.org/10.1139/t06-078>.
- Wang, H., Koseki, J., Sato, T., Chiaro, G. and Tan Tian, J. (2016), "Effect of saturation on liquefaction resistance of iron ore fines and two sandy soils", *Soils Found.*, **56**(4), 732-44. <https://doi.org/10.1016/j.sandf.2016.07.013>.
- Whittle, A.J., El-Naggar, H.M., Aky, S.A.Y. and Galaa, A.M. (2022), "Stability analysis of upstream tailings dam using numerical limit analyses", *J. Geotech. Geoenviron. Eng.*, **148**(6). [https://doi.org/10.1061/\(ASCE\)GT.1943-5606.0002792](https://doi.org/10.1061/(ASCE)GT.1943-5606.0002792).
- Zeybek, A. (2022), "Experimental and empirical studies to evaluate liquefaction resistance of partially saturated sands", *Appl. Sci.*, **13**(81), 1-23. <https://doi.org/10.3390/app13010081>.
- Zhang, B., Muraleetharan, K.K. and Liu, C. (2016), "Liquefaction of unsaturated sands", *Int. J. Geomech.*, **16**(6), 1-8. [https://doi.org/10.1061/\(ASCE\)GM.1943-5622.0000605](https://doi.org/10.1061/(ASCE)GM.1943-5622.0000605).
- Zuoan, W., Yulong C., Guangzhi, Y., Yonghao, Y. and Weimin, S. (2019), "An alternative upstream method for the Zhelamuqing tailings impoundment construction of a Copper Mine in China", *Geomech. Eng.*, **19**(5), 383-392. <https://doi.org/10.12989/gae.2019.19.5.383>.